Available online at www.sciencedirect.com

ScienceDirect

IFAC PapersOnline CONFERENCE PAPER ARCHIVE

IFAC PapersOnLine 55-22 (2022) 183–188

LQR-based MIMO PID control of a 2-DOF helicopter system with uncertain cross-coupled gain

Falguni Gopmandal, Arun Ghosh

Electrical Engineering Department, IIT Kharagpur, West Bengal, India-721302.

(e-mails: falgun.ece@gmail.com; arunghosh1@gmail.com)

Abstract: This work deals with designing multi-input multi-output (MIMO) proportional-integral-derivative (PID) controllers to achieve linear quadratic (LQ) performance of a laboratory-based two degree-of-freedom (2-DOF) helicopter system with norm-bounded uncertainties in the cross-coupled gain. It is shown that, for such an uncertain system, the MIMO PID design problem can be recast as a full-state feedback control for an augmented uncertain system. Consequently, a simple linear matrix inequality problem is solved to determine the PID parameters in order to achieve robust LQ performance. The efficacy of the proposed controller is shown through extensive simulations and experiments.

Keywords: MIMO PID control, 2-DOF helicopter, norm-bounded uncertainty.

1. INTRODUCTION

The laboratory-based two degree-of-freedom (2-DOF) helicopter system is a benchmark multivariable unstable system with strong cross-coupling. It is an ideal system to assess the performance of a multivariable or multi-input multi-output (MIMO) controller. Numerous decentralized or multi-loop control schemes have been proposed for this system; see Hernandez-Gonzalez et al. (2012); Wen and Lu (2008); Goyal et al. (2020) and the references therein. However, the system being highly coupled, such controllers yield poor performance in general. To get rid of the coupling, the centralized multivariable controller in Pradhan and Ghosh (2013) has been designed via open-loop decoupling method. Besides being a polynomial-based approach, in this method, however, the controller order becomes high. Several other advanced control techniques like $\mathcal{H}_\infty$ control, fuzzy control, predictive control, adaptive control, sliding mode control, neural network control, feedback linearizing control, etc., have also been employed; see López-Martínez et al. (2020); Mendez-Monroy and Benitez-Perez (2012); Dutka et al. (2020); Nuthi and Subbarao (2015); Gao et al. (2016); Boukadida et al. (2019); Sadala and Patre (2018); Zhao et al. (2022); Lopez-Martinez and Rubio (2003). However, the majority of these controllers have complicated structures and are of higher order. Therefore, it is desirable to design a low order MIMO controller that can achieve satisfactory performance and robustness.

As is well known, proportional-integral-derivative (PID) controllers are of low order and easy to implement in both analog and digital settings [Ang et al. (2005)]. In literature, a lot of efforts have been put in the area of (centralized) MIMO PID control design; see Mattei (2001); Lin et al. (2004); Bianchi et al. (2008); Pradhan and Ghosh (2015); Gopmandal and Ghosh (2021); Pradhan and Ghosh (2022) and references therein. In most of the methods, the MIMO PID design problem is handled by transforming it into a static output feedback (SOF) problem. In Pradhan and Ghosh (2015), a class of plants for which this SOF problem becomes complete state feedback problem is obtained and nominal linear quadratic (LQ) performance is achieved. Recently in Pradhan and Ghosh (2022), the MIMO PID controller is designed not only to achieve LQ performance under nominal condition, but in presence of norm-bounded parametric uncertainties in the plant as well. However, the inclusion of derivative filter dynamics in the controller design makes this approach iterative, even for the class of plants as mentioned above. Moreover, in this method, one positive scalar parameter, namely ϵ, which arises due to presence of norm-bounded uncertainties, has to be chosen a priori. Naturally it is interesting to see if these problems can be avoided with ideal PID controllers, at least for the class of plants for which ideal PID design becomes equivalent to the complete state feedback problem, as identified in Pradhan and Ghosh (2015).

In this paper, we attempt to solve the above problem for a laboratory-based 2-DOF helicopter system. For simplicity, we consider the norm-bounded uncertainties in the cross-coupled gain only. This system being in the class as mentioned in the above paragraph, it is shown that the MIMO PID design here can be transformed into a full-state feedback control for an augmented uncertain system. As a result, the PID gains can be computed by directly solving a linear matrix inequality (LMI) in order to achieve robust LQ performance. The PID controller thus designed is also implemented on the physical setup. Extensive simulations and experiments are carried out to compare its performance with the PID control designed to achieve only nominal LQ performance.

The rest of the paper is organized as follows. In Section 2, the state-space model of the system is obtained. Next, the

10.1016/j.ifacol.2023.03.031

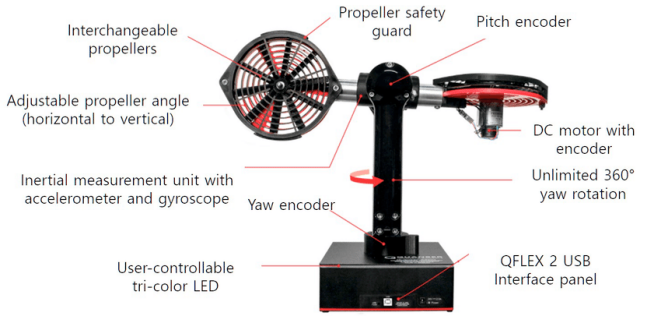

Fig. 1. Quanser 2-DOF helicopter setup.

MIMO PID design methodology is described in Section 3. The simulations and experimental results are presented in Section 4. Finally, the conclusions are drawn in Section 5.

2. SYSTEM DESCRIPTION

The laboratory-based helicopter model to be used is shown in Fig. 1. It is manufactured by Quanser Inc, Canada. Unlike the normal helicopter model which has 3-DOF motions (namely, pitch, yaw, roll), it has 2-DOF motions (pitch and yaw) [see Inc. (2016)]. In this setup, the motion about the pitch axis is controlled by the front rotor, which is horizontal to the ground, whereas the motion about the yaw axis is controlled by the back or tail rotor. While in a normal helicopter, maneuvering is obtained by tilting the rotor blade angle, in this setup, the same is carried out by changing the speed of the motors. The high-resolution encoders are used to measure the pitch and yaw angles.

2.1 Modelling

The free-body diagram of the system is shown in Fig. 2. In this figure, F_p is the aerodynamic force acting on the pitch rotor and the corresponding torque τ_p about the pivot causes angular motion θ in pitch plane. Similarly the aerodynamic force F_y causes torque τ_y which in turn creates angular motion ψ in yaw plane. Again, because of the self-rotational motion of pitch rotor a cross-torque is produced, which prevents the yaw motion. Similarly, the cross-torque produced by the yaw rotor rotational motion prevents the pitch motion. These cross-torques cause significant cross-coupling between pitch and yaw channels. In Inc. (2016), a simple spring-mass-damper type of linear model that takes this coupling into account, is considered. The equations of motion are described by

$$J_p\ddot{\theta} + D_p\dot{\theta} + K_{sp}\theta = \tau_p,\ J_y\ddot{\psi} + D_y\dot{\psi} = \tau_y \qquad (1)$$

where τ_p, τ_y are related to their respective motor voltages by

$$\tau_p = K_{pp}V_p + K_{py}V_y,\ \tau_y = K_{yp}V_p + K_{yy}V_y. \qquad (2)$$

Table 1 lists the model parameters and their respective values. In above, the term K_{sp} is because of the gravitational force acting on the vertical (i.e., pitch) motion. The yaw motion being in the horizontal plane, no such term is considered there. This makes the system to have a pole at $s = 0$. It is noteworthy that in the above modelling, the coupling between pitch and yaw motions is represented by the cross-terms K_{py} and K_{yp}. As $|K_{py}| \approx 2|K_{pp}|$, but $|K_{yp}| \approx |K_{yy}|$ (see Table 1), the coupling from V_y to θ is significantly more than the one from V_p to ψ.

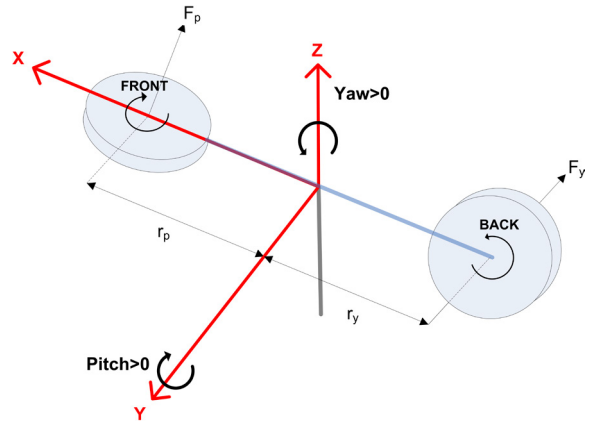

Fig. 2. Free-body diagram.

Table 1. System parameters.

Parameters	Value/range
Moment of inertia about pitch axis (J_p)	0.0219 kgm^2
Moment of inertia about yaw axis (J_y)	0.0220 kgm^2
Damping about pitch axis (D_p)	0.00711 Vs/rad
Damping about yaw axis (D_y)	0.0220 Vs/rad
Stiffness about pitch axis (K_{sp})	0.0375 Nm/rad
Torque thrust gain from pitch rotor (K_{pp})	0.0011 Nm/V
Torque thrust gain from yaw rotor (K_{yy})	0.0022 Nm/V
Cross-torque thrust gain acting on pitch rotor from yaw rotor (K_{py})	0.0021 Nm/V
Cross-torque thrust gain acting on yaw rotor from pitch rotor (K_{yp})	−0.0027 Nm/V
Voltage applied to pitch rotor (V_p)	±24 V
Voltage applied to yaw rotor (V_y)	±24 V

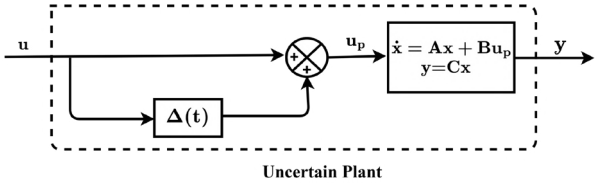

Fig. 3. Representation of the system with cross-coupled uncertainties.

Now, consider the state vector $x = [\theta \quad \psi \quad \dot{\theta} \quad \dot{\psi}]^T$, control input $u_p = [V_p \quad V_y]^T$ and output $y = [\theta \quad \psi]^T$. Then from (1), (2), the state-space representation of the system becomes

$$\dot{x} = Ax + Bu_p,\ y = Cx \qquad (3)$$

where,

$$A = \begin{bmatrix} 0 & 0 & 1 & 0 \\ 0 & 0 & 0 & 1 \\ -K_{sp}/J_p & 0 & -D_p/J_p & 0 \\ 0 & 0 & 0 & -D_y/J_y \end{bmatrix},$$

$$B = \begin{bmatrix} 0 & 0 \\ 0 & 0 \\ K_{pp}/J_p & K_{py}/J_p \\ K_{yp}/J_y & K_{yy}/J_y \end{bmatrix}, C = \begin{bmatrix} 1 & 0 & 0 & 0 \\ 0 & 1 & 0 & 0 \end{bmatrix}. \qquad (4)$$

Next, to explicitly consider the uncertainties in cross-coupled gain we add a full-block, time-varying uncertainty $\Delta(t)$ as shown in Fig. 3, where

$$\Delta(t) = \begin{bmatrix} \delta_{11}(t) & \delta_{12}(t) \\ \delta_{21}(t) & \delta_{22}(t) \end{bmatrix},\ \|\Delta(t)\|_2 \leq \delta. \qquad (5)$$

Then, the uncertain system shown in Fig. 3 becomes

$$\dot{x} = Ax + B[I + \Delta(t)]u,\ y = Cx. \tag{6}$$

The above system can be represented in standard form [see Petersen and Tempo (2014)] as

$$\dot{x} = Ax + [B + D\Delta_B(t)E]u,\ y = Cx \tag{7}$$

where, $D = B,\ E = \delta I_2$ and $\Delta_B(t)$ is a norm-bounded time-varying uncertain matrix satisfying $\|\Delta_B(t)\|_2 \leq 1$.

3. MIMO PID CONTROL DESIGN

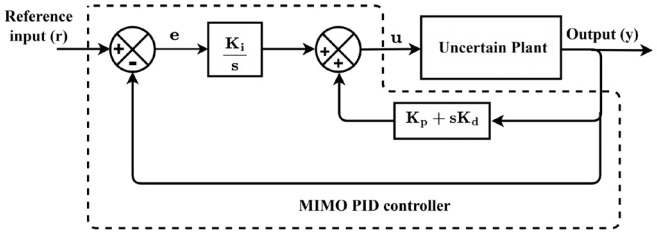

Fig. 4. MIMO PID controller.

The MIMO PID controller to be used for the uncertain plant (7) is shown in Fig. 4. The control law is

$$u = K_p y + K_d \frac{dy}{dt} + K_i \int_0^t (r - y)dt \tag{8}$$

where $K_p, K_i, K_d \in \mathbb{R}^{2\times 2}$. It may be noted that the above controller structure is I-PD type, where the PD part is kept in the feedback path and I-part in the forward path. As is well known, the PD part in the feedback path eliminates the derivative and proportional kicks on output and control input, which occur in case of a standard parallel PID controller, when a step reference input is applied. The I-PD structure also makes the PID controller 2-DOF in nature, which helps one achieve improved r-to-y and r-to-u responses as compared to the standard (i.e., 1-DOF) PID structure; see Ang et al. (2005). Moreover, the I-PD structure helps one transform the controller into a state feedback control, as presented next. The presence of pure derivative part, however, makes the feedback system prone to measurement noise. Also, the same being improper, it is difficult to implement. To this end, a derivative filter is employed in cascade with the derivative gain K_d, which is given by

$$F(s) = \frac{1}{\tau_d s + 1} I_2 \tag{9}$$

where the filter time constant is chosen as $\tau_d << \|K_d\|_2/\|K_p\|_2$, so that it does not affect the behaviour of the ideal PID control much Skogestad and Postlethwaite (2007).

3.1 State feedback transformation of the control law

In this section, it is shown that the MIMO PID design for the uncertain system (7) can be transformed into a state feedback design for an augmented uncertain system.

Let, $\xi = \int_0^t (r-y)dt$. As $y = [\theta \quad \psi]^T$, one has $\dot{y} = [\dot{\theta} \quad \dot{\psi}]^T$. Then, the control law in (8) can be rewritten as

$$u = [K_p\ K_d\ K_i] \begin{bmatrix} \theta \\ \psi \\ \dot{\theta} \\ \dot{\psi} \\ \xi \end{bmatrix} \implies u = K_{PID}\bar{x} \tag{10}$$

where,

$$K_{PID} = [K_p\ K_d\ K_i],\ \bar{x} = [x^T\ \xi^T]^T. \tag{11}$$

Next, augmenting ξ with x, the augmented system becomes

$$\dot{\bar{x}} = \bar{A}\bar{x} + \bar{B}(t)u + Gr,\ y = \bar{C}\bar{x} \tag{12}$$

where,

$$\bar{A} = \begin{bmatrix} A & 0_{4\times 2} \\ -C & 0_{2\times 2} \end{bmatrix},\ \bar{B}(t) = \bar{B}_0 + \bar{D}\Delta_B(t)\bar{E},\ G = \begin{bmatrix} 0_{4\times 2} \\ I_2 \end{bmatrix},$$

$$\bar{C} = [C\ 0_{2\times 2}],\ \bar{B}_0 = \begin{bmatrix} B \\ 0_{2\times 2} \end{bmatrix},\ \bar{D} = \begin{bmatrix} D \\ 0_{2\times 2} \end{bmatrix},\ \bar{E} = E. \tag{13}$$

Now, the control law (10) can be thought of as a state feedback control law for the augmented uncertain system (12). Thus, designing the gains K_p, K_i, K_d for the original uncertain system (7) becomes the design of state feedback gain K_{PID} for the augmented uncertain system (12).

3.2 Robust LQ performance

In this section, an LMI-based method is given to design the state feedback gain K_{PID} for the uncertain augmented plant (12), such that some LQ performance is achieved. To this end, we assume the pair $(\bar{A}, \bar{B}_0)$ stabilizable and consider the LQR cost as

$$J = \int_0^\infty (\bar{x}^T Q\bar{x} + u^T Ru)dt,\ Q \in \mathbb{R}^{6\times 6}, R \in \mathbb{R}^{2\times 2} \tag{14}$$

with $Q = Q^T > 0,\ R = R^T > 0$ and initial state $\bar{x}(0) = \bar{x}_0$. Then, the gain K_{PID} can be determined following the result given below.

***Proposition** 1.* The feedback system consisting of the uncertain plant (7) and the PID controller (8) is quadratically stable[1] with cost $J < \gamma$ iff there exist matrices $\bar{P} = \bar{P}^T > 0$, Y of appropriate dimensions and a real scalar $\epsilon > 0$ such that the following LMIs hold:

$$\begin{bmatrix} \mathrm{Sym}(\bar{A}\bar{P} + \bar{B}_0 Y) + \epsilon\bar{D}\bar{D}^T & \bar{P} & Y^T & (\bar{E}Y)^T \\ \bar{P} & -Q^{-1} & 0 & 0 \\ Y & 0 & -R^{-1} & 0 \\ \bar{E}Y & 0 & 0 & -\epsilon I \end{bmatrix} \leq 0 \tag{15}$$

$$\begin{bmatrix} \gamma & \bar{x}_0^T \\ \bar{x}_0 & \bar{P} \end{bmatrix} \geq 0. \tag{16}$$

where $\mathrm{Sym}(X)$ means $X + X^T$. Then, K_{PID} becomes

$$K_{PID} = Y\bar{P}^{-1}. \tag{17}$$

***Proof of Proposition** 1.* Here S_0 of Pradhan and Ghosh (2022) becomes identity matrix. Therefore, on substituting $K_{PID}\bar{P} = Y$, the bilinear matrix inequality (BMI) in Theorem 2 of Pradhan and Ghosh (2022) becomes LMI. Also, as no uncertainty is considered in the state matrix A, the matrix $\bar{E}_1$ of Theorem 2 of Pradhan and Ghosh

[1] A time-varying system $\dot{x}(t) = f(x(t), t)$ is quadratically stable if there exists a constant matrix $P = P^T > 0$ such that with Lyapunov function $V(x(t)) = x(t)^T Px(t)$, $x(t) \neq 0$, the system satisfies $\dot{V}(x(t)) < V(x(t))$, $\forall\ t$; see Petersen and Tempo (2014).

(2022) is set to zero in this case. Finally, (17) follows from the relation $K_{PID}\bar{P} = Y$.

***Remark** 1.* If there is no uncertainty, i.e., $\delta = 0$, then one may consider $\bar{D} = 0, \bar{E} = 0$. Therefore the LMI (15) is satisfied for any $\epsilon > 0$. This implies, for nominal LQR performance design, it suffices to consider the first 3×3 block of the LMI (15) with $\bar{D} = 0$.

3.3 Some design details

In this section, we first present some numerical details of the proposed PID design that achieves robust LQ performance. Numerical details are also provided for the PID design that achieves only nominal LQ performance. The latter results will be used for performance comparison in Section 4.

To ensure robust LQ performance, we set the uncertainty limit as $\delta = 0.7$. Next, the LQR weights for the system (12) are chosen as $Q = \text{diag}\{30, 30, 1, 1, 200, 200\}$, $R = \text{diag}\{0.001, 0.001\}$. Note, in order to reduce tracking error, more weight is given on ξ. Further, to reduce the overshoot, some weights are put on θ and ψ. The derivatives of outputs, i.e., $\dot{\theta}, \dot{\psi}$ are given comparatively less weights. The weight R is chosen to keep the control voltage well within ± 24 V. Further, to give more emphasis on the tracking error, the initial state of the augmented system is taken as $\bar{x}_0 = [0, 0, 0, 0, 1, 1]^T$. With these settings, the optimal PID gains are obtained following Proposition 1 as

$$K_p = \begin{bmatrix} -367.17 & 481.28 \\ -326.86 & -185.02 \end{bmatrix}, \; K_d = \begin{bmatrix} -137.13 & 134.38 \\ -124.65 & -53.26 \end{bmatrix}$$
$$K_i = \begin{bmatrix} 484.12 & -605.31 \\ 415.51 & 212.58 \end{bmatrix}. \quad (18)$$

Finally, as $\|K_d\|_2/\|K_p\|_2 = 0.3330$, we choose the derivative filter time-constant $\tau_d = 0.0333$ s.

Next, the MIMO PID controller is designed to achieve LQ performance for the nominal plant (i.e., with $\delta = 0$) only. To this end, the LQR weights are kept same as before, so that the nominal responses become similar. In this case, the optimal PID gains are obtained following Remark 2 as

$$K_p = \begin{bmatrix} -328.61 & 400.42 \\ -279.25 & -143.36 \end{bmatrix}, \; K_d = \begin{bmatrix} -77.51 & 77.20 \\ -69.01 & -30.52 \end{bmatrix}$$
$$K_i = \begin{bmatrix} 529.50 & -649.27 \\ 420.10 & 205.06 \end{bmatrix}. \quad (19)$$

As $\|K_d\|_2/\|K_p\|_2 = 0.2190$, here, we choose $\tau_d = 0.0219$ s.

4. SIMULATION AND EXPERIMENTAL RESULTS

In this section, we study the behaviour of both the nominal and robust PID designs through simulations and experiments. The real-time implementation diagram of the controller is shown in Fig. 5. The controller is implemented on MATLAB/Simulink (2021b) of the computer and the built-in data acquisition (DAQ) card with sampling rate of 500 Hz is used to interface with the physical system via QFLEX 2 USB.

4.1 Frequency response study

To study the behaviour of the compensated system using frequency response, we consider sensitivity function $S(s)$, complementary sensitivity function $T(s)$, and control sensitivity function $S(s)K(s)$, where $S(s) = [I + L(s)]^{-1}$, $T(s) = L(s)[I+L(s)]^{-1}, L(s) = K(s)P(s)$ with $P(s)$ being the plant and $K(s)$ the PID controller (along with filter). It is well known that $\|S\|_\infty$ is a measure of robustness against parameter variations and $\|T\|_\infty$ is a measure of robustness against worst-case multiplicative type unmodelled dynamics of the plant. On the other hand, $\|SK\|_\infty$ is used as a measure of maximum control input magnitude as well as a measure for robustness against unmodelled additive type uncertainties; see Skogestad and Postlethwaite (2007).

Table 2. Robustness margins for the uncertain plant.

PID control method	$\|S\|_\infty$	$\|T\|_\infty$	$\|SK\|_\infty$
Proposed robust LQ control	1.67	1.38	3.34
Nominal LQ control	2.18	2.07	11.22

To see the performance in presence of uncertainty, 50 randomly chosen plants $P(s)$ are taken from the considered uncertainty set. The proposed as well as nominal PID controller have been employed for all these sample plants. The singular value plots are shown in Figs. 6, 7, 8. The peaks of those plots are mentioned in Table 2. It clearly shows that with robust PID control, these magnitudes, in particular $\|SK\|_\infty$, are much less as compared to the nominal PID design, as expected. The large value of $\|SK\|_\infty$ of the nominal PID signifies that it is very much sensitive to uncertainties in cross-coupled gain. Also, it is seen from Figs. 6, 7 that with both the designs, the low frequency magnitude of S plot and high frequency magnitude of T plot are more or less same. This implies that the disturbance and noise attenuation capability of the robust PID is not deteriorated w.r.t the nominal PID.

4.2 Time response

The real-time responses for both the robust and nominal LQ performance-based PID designs are shown in Figs. 9, 10. Here, to create a worse situation, we consider $\delta_{11} = \delta_{12} = \delta_{21} = \delta_{22} = -0.3$ (which satisfies $\delta = 0.6$). Fig. 10-(a) shows that the response with the nominal LQ performance-based PID control deviates significantly from the unperturbed one, when the uncertainty in the cross-coupled gain occurs. On the other hand, as shown in Fig. 9-(a), the perturbed responses with the proposed robust LQ performance-based PID design remains close to the unperturbed one, as expected. From Fig. 10-(b), it is clear for the case of nominal LQ performance-based PID design that, when the yaw command is changed, because of the cross-coupling effect, V_p saturates for some time duration (see in between 10 and 15 s and at 25 s), which in turn causes significant deviations in the perturbed outputs from the unperturbed ones. Note, as can be seen from Fig. 9-(b), for the robust LQ performance-based PID design, the above saturation occurs for comparatively

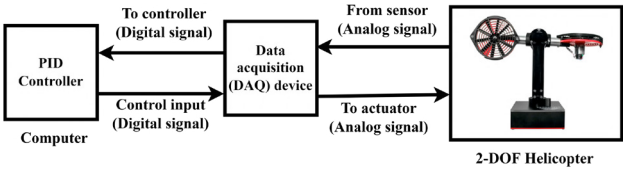

Fig. 5. Real-time implementation diagram.

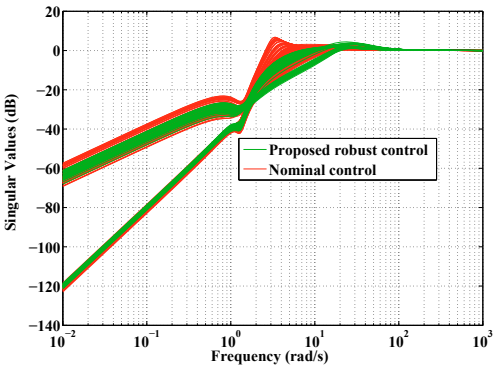

Fig. 6. Singular value plot of S.

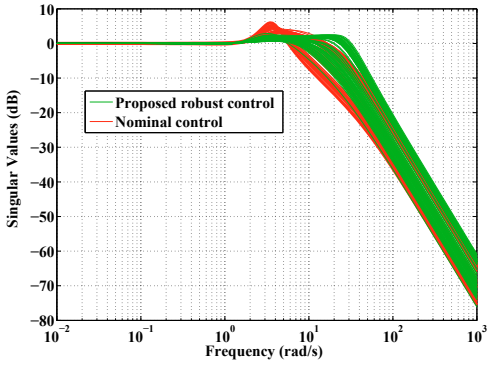

Fig. 7. Singular value plot of T.

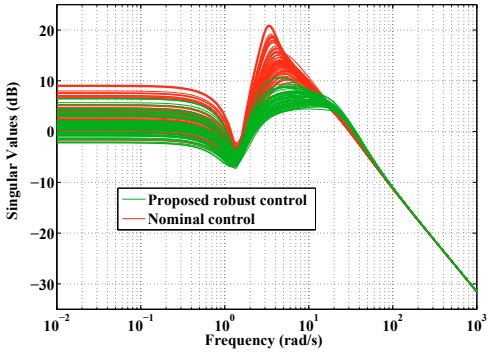

Fig. 8. Singular value plot of SK.

small duration of time in between 10 and 15 s, which results in minute deviation of the perturbed outputs. Note, as already mentioned in the paragraph above (3), the coupling from the other way is not that much significant.

5. CONCLUSIONS

In this paper, an LQR-based MIMO PID controller has been designed for a laboratory-based 2-DOF helicopter system with uncertain cross-coupled gain. The design has been carried out by first transforming the problem into a state feedback control for an augmented uncertain system and then computing the state feedback gains by solving an LMI problem, so that robust LQ performance is achieved. For comparison, a nominal LQR-based MIMO

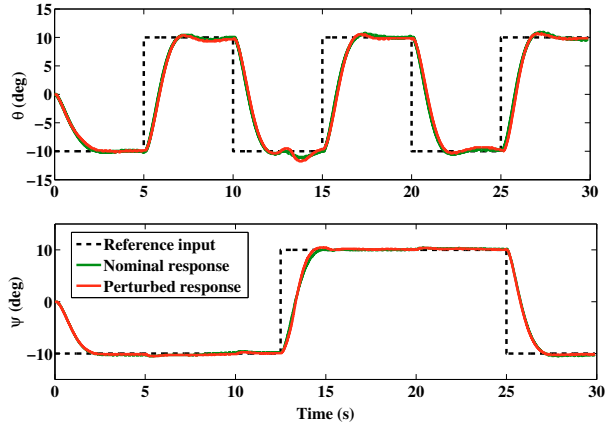

(a) Output.

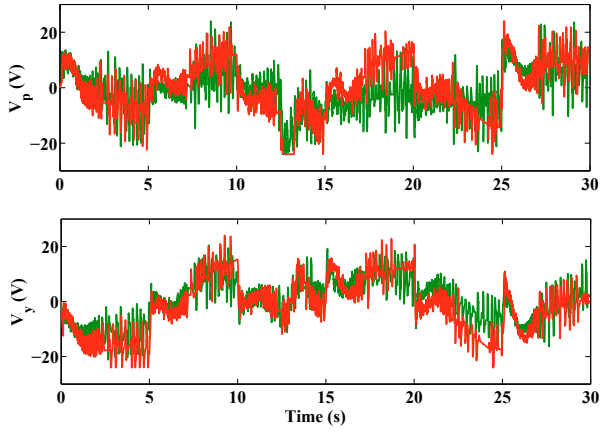

(b) Control input.

Fig. 9. Responses with the robust LQ optimal MIMO PID controller (real-time).

PID controller has also been designed following the same approach. Both the controllers have been implemented in real-time. The simulation and experimental results show that, in presence of uncertainties, the behaviour of the PID controller designed to achieve robust LQ performance is much superior to the one designed to achieve only the nominal LQ performance, as expected.

ACKNOWLEDGEMENTS

The authors acknowledge the financial support from Science and Engineering Research Board (SERB), New Delhi, India, through the sponsored project with Project No. CRG/2020/00843, to carry out this research.

REFERENCES

Ang, K.H., Chong, G., and Li, Y. (2005). PID control system analysis, design, and technology. *IEEE Transactions on Control Systems Technology*, 13(4), 559–576.

Bianchi, F.D., Mantz, R.J., and Christiansen, C.F. (2008). Multivariable PID control with set-point weighting via BMI optimisation. *Automatica*, 44(2), 472–478.

Boukadida, W., Benamor, A., Messaoud, H., and Siarry, P. (2019). Multi-objective design of optimal higher

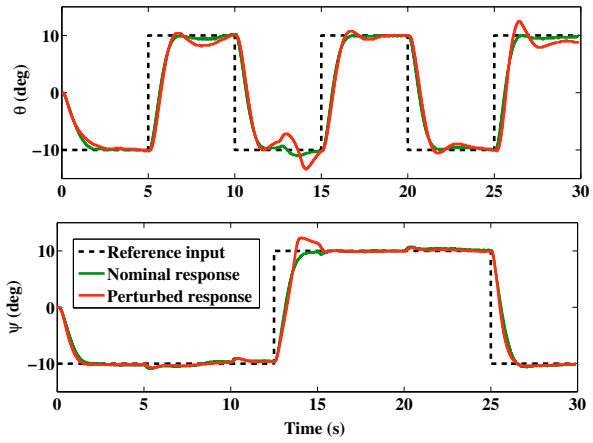

(a) Output.

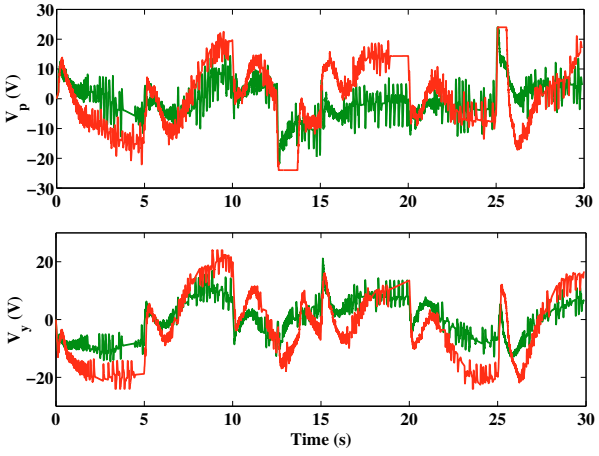

(b) Control input.

Fig. 10. Responses with LQ optimal MIMO PID controller (real-time).

order sliding mode control for robust tracking of 2-DOF helicopter system based on metaheuristics. *Aerospace Science and Technology*, 91, 442–455.

Dutka, A.S., Ordys, A.W., and Grimble, M.J. (2020). Nonlinear predictive control of 2 DOF helicopter model. *Proceedings of the 42nd IEEE International Conference on Decision and Control, 3954–3959.*

Gao, W., Huang, M., Jiang, Z.P., and Chai, T. (2016). Sampled-data-based adaptive optimal output-feedback control of a 2-degree-of-freedom helicopter. *IET Control Theory & Applications*, 10(12), 1440–1447.

Gopmandal, F. and Ghosh, A. (2021). A hybrid search based H_∞ synthesis of static output feedback controllers for uncertain systems with application to multivariable PID control. *International Journal of Robust and Nonlinear Control*, 31(12), 6069–6090.

Goyal, J.K., Aggarwal, S., Ghosh, S., Kamal, S., Dworak, P., Singh, B., and Pal, A.K. (2020). Experimental design of robust decentralized PI controller for TRMS through polytopic modeling. *Proceedings of the IEEE International Conference on Industrial Technology, 47–52.*

Hernandez-Gonzalez, M., Alanis, A.Y., and Hernández-Vargas, E.A. (2012). Decentralized discrete-time neural control for a quanser 2-DOF helicopter. *Applied Soft Computing*, 12(8), 2462–2469.

Inc., Q. (2016). Quanser aero laboratory guide. *Technical Report, ON, Canada.*

Lin, C., Wang, Q.G., and Lee, T.H. (2004). An improvement on multivariable PID controller design via iterative LMI approach. *Automatica*, 40(3), 519–525.

Lopez-Martinez, M. and Rubio, F.R. (2003). Control of a laboratory helicopter using feedback linearization. *Proceedings of the European Control Conference (ECC), 3430–3435.*

López-Martínez, M., Vivas, C., and Ortega, M.G. (2020). A multivariable nonlinear H_∞ controller for a laboratory helicopter. *Proceedings of the 44th IEEE Conference on Decision and Control, 4065–4070.*

Mattei, M. (2001). Robust multivariable PID control for linear parameter varying systems. *Automatica*, 37(12), 1997–2003.

Mendez-Monroy, P. and Benitez-Perez, H. (2012). Fuzzy control with estimated variable sampling period for nonlinear networked control systems: 2-DOF helicopter as case study. *Transactions of the Institute of Measurement and Control*, 34(7), 802–814.

Nuthi, P. and Subbarao, K. (2015). Experimental verification of linear and adaptive control techniques for a two degrees-of-freedom helicopter. *Journal of Dynamic Systems, Measurement, and Control*, 137(6), 064501.

Petersen, I.R. and Tempo, R. (2014). Robust control of uncertain systems: Classical results and recent developments. *Automatica*, 50(5), 1315–1335.

Pradhan, J.K. and Ghosh, A. (2015). Multi-input and multi-output proportional-integral-derivative controller design via linear quadratic regulator-linear matrix inequality approach. *IET Control Theory & Applications*, 9(14), 2140–2145.

Pradhan, J.K. and Ghosh, A. (2013). Design and implementation of decoupled compensation for a twin rotor multiple-input and multiple-output system. *IET Control Theory & Applications*, 7(2), 282–289.

Pradhan, J.K. and Ghosh, A. (2022). Multivariable robust proportional-integral-derivative control for linear quadratic compensation of a class of norm-bounded uncertain systems. *Journal of Dynamic Systems, Measurement, and Control*, 144(10), 101003.

Sadala, S. and Patre, B. (2018). A new continuous sliding mode control approach with actuator saturation for control of 2-DOF helicopter system. *ISA Transactions*, 74, 165–174.

Skogestad, S. and Postlethwaite, I. (2007). *Multivariable feedback control: Analysis and design*, volume 2. Wiley New York.

Wen, P. and Lu, T.W. (2008). Decoupling control of a twin rotor MIMO system using robust deadbeat control technique. *IET Control Theory & Applications*, 2(11), 999–1007.

Zhao, Z., Zhang, J., Liu, Z., Mu, C., and Hong, K.S. (2022). Adaptive neural network control of an uncertain 2-DOF helicopter with unknown backlash-like hysteresis and output constraints. *IEEE Transactions on Neural Networks and Learning Systems.* (Early Acess).